Inorg. Chem. **2004**, *43*, 317–323

A Facile Route to Bimetallic Ruthenium Dipyridophenazine Complexes

Clive Metcalfe, Ihtshamul Haq,† and Jim A. Thomas*

Department of Chemistry, University of Sheffield, Sheffield S3 7HF, U.K.

Received July 1, 2003

Using achiral coordinatively unsaturated metal complex building-blocks, the two step synthesis of a bimetallic complex containing independent [Ru^{II}dppz] units tethered together by a linking 4,4′dipyridyl-1,5-pentane ligand is reported. Photophysical studies on this prototype system indicate that the characteristic luminescence of the [Ru^{II}dppz] moieties is perturbed by self-quenching processes. Preliminary binding studies on the complex with natural and synthetic duplex DNA is reported. Luminescence and calorimetric titrations reveal that the complex does not show enhanced binding affinity with respect to analogous monometallic complexes. This result is interpreted by a consideration of the length and rigidity of the linker employed in the complex.

Introduction

Polypyridyl d^6 metal complexes are extensively investigated as their rich photophysical and redox properties makes them potentially useful in a range of applications such as; light harvesting,[1] electron transfer,[2] and probes for biological systems,[3] particularly nucleic acids.[4] In this context, the DNA binding properties of $[Ru(phen)_2(dppz)]^{2+}$, **1**, (dppz = dipyrido[3,2-*a*:2′,3′-*c*]phenazine, phen = 1,10-phenanthroline), Scheme 1, has attracted particular attention.[5] Although the exact orientation of the complex when bound to DNA has been open to much discussion, it is widely accepted that intercalation of the dppz ligand into the DNA base stack forms the basis of interaction.[5,6] The binding process can be monitored using UV/visible spectroscopy as intercalation results in large hypochromic shifts in the absorption bands of the complex. Luminescence offers a further means of monitoring binding: in what has become known as the DNA light switch effect, emission from aqueous solutions of **1** is quenched by water molecules, while binding to DNA enhances luminescence by several orders of magnitude.[5a,6,7] In an attempt to construct new architectures for metallo-intercalators, we have been investigating the properties of $[Ru(tpm)(L)(dppz)]^{2+}$ (where tpm = tris-(1-pyrazolyl)-methane, L = N-donor ligand); see Scheme 1. Initial work on monometallic complexes[8] has shown that their DNA binding parameters compare favorably with those of **1**.

More recently, in an attempt to increase the binding affinity and DNA sequence recognition properties of such complexes bimetallic systems have been investigated. For example, Kelly and co-workers have demonstrated that dimers composed of linked nonintercalative metal centers, such as $[(bpy)_2Ru(Mebpy)(CH_2)_5(bpyMe)Ru(bpy)_2]^{4+}$, **3** (where bpy = 2,2′bipyridine, MeBpy = 4-methyl-2,2′-bipyridyl-4′-), Scheme 1, show greatly enhanced binding to DNA over their monometallic analogues.[9] Nordén, et al. have synthesized bimetallic complexes **4** and **5**, connected via dppz moieties, that intercalate via a threading mechanism, resulting in high-affinity DNA binding.[10] However, the multistep synthesis of these latter systems, starting from coordinatively saturated, classically resolved chiral metal complexes, is not trivial.

Complexes related to **2** are convenient building blocks for the construction of analogous systems as they are achiral and are coodinatively unsaturated, thus offering more facile

* Corresponding author. Fax: International code + (114) 273-8673. E-mail: james.thomas@sheffield.ac.uk.
† E-mail: I.Haq@sheffield.ac.uk.

(1) (a) Balzani, V.; Ceroni, P; Juris, A.; Venturi, M.; Campagna, S.; Puntoreiro, F.; Serroni, S. *Chem. Rev.* **1996**, *96*, 759. (b) Balzani, V.; Juris, A.; Venturi, M.; Campagna, S.; Serroni, S. *Coord. Chem. Rev.* **2001**, 545.
(2) (a) Demadis, K. D.; Hartshorn, C. M.; Meyer, T. J. *Chem. Rev.* **2001**, *101*, 2655. (b) Brunschwig, B.; Creutz, C.; Sutin, N. *Chem. Soc. Rev.* **2002**, *31*, 168.
(3) Telford, J. R.; Wittung-Stafshede, P.; Gray, H. B.; Winkler, J. R. *Acc. Chem. Res.* **1998**, *31*, 755.
(4) (a) Nordén, B.; Lincoln, P.; Akerman, B.; Tuite, E. In *Metal Ions in Biological Systems*; Sigel, H., Sigel, A., Eds.;, Marcel Dekker: New York, **1996**; Vol. 33; 177. (b) Erkkila, K. E.; Odom, D. T.; Barton, J. K. *Chem. Rev.* **1999**, *99*, 2777. (c) Metcalfe, C.; Thomas, J. A. *Chem. Soc. Rev.* **2003**, *32*, 214.
(5) See for example: (a) Friedman, A. E.; Chambron, J.-C.; Sauvage, J.-P.; Turro, N. J.; Barton, J. K. *J. Am. Chem. Soc.* **1990**, *112*, 4960. (b) Hiort, C.; Lincoln, P.; Nordén, B. *J. Am. Chem. Soc.* **1993**, *115* 3448. (c) Tuite, E.; Lincoln, P.; Nordén, B. *J. Am. Chem. Soc.* **1997**, *119*, 239. (d) Holmlin, R. E.;. Stemp, E. D. A.; Barton, J. K. *Inorg. Chem.* **1998**, *37*, 29.
(6) Jenkins, Y.; Friedman, A. E.; Turro, N. J.; Barton, J. K. *Biochemistry* **1992**, *31*, 10809.
(7) (a) Friedman, A. E.; Kumar, C. P.; Turro, N. J.; Barton, J. K. *Nucleic Acid Res.* **1991**, *19*, 2595. (b) Hartshorn, R. M.; Barton, J. K. *J. Am. Chem. Soc.* **1992**, *114*, 5919.
(8) Metcalfe, C.; Adams, H.; Haq, I. *Chem. Commun.* **2003**, 1152.
(9) (a) O'Reilly, F.; Kelly, J.; Kirsch-De Mesmaeker, A.; *Chem. Commun.* **1995**, 1013. (b) O'Reilly, F.; Kelly, J. *New J. Chem.* **1998**, 215. (c) O'Reilly, F.; Kelly, J. *J. Phys. Chem B* **2000**, *104*, 7206.

10.1021/ic034749x CCC: $27.50
Published on Web 12/12/2003

Scheme 1. Monometallic (A) and Bimetallic (B) Metallointercalators Relevant to This Work

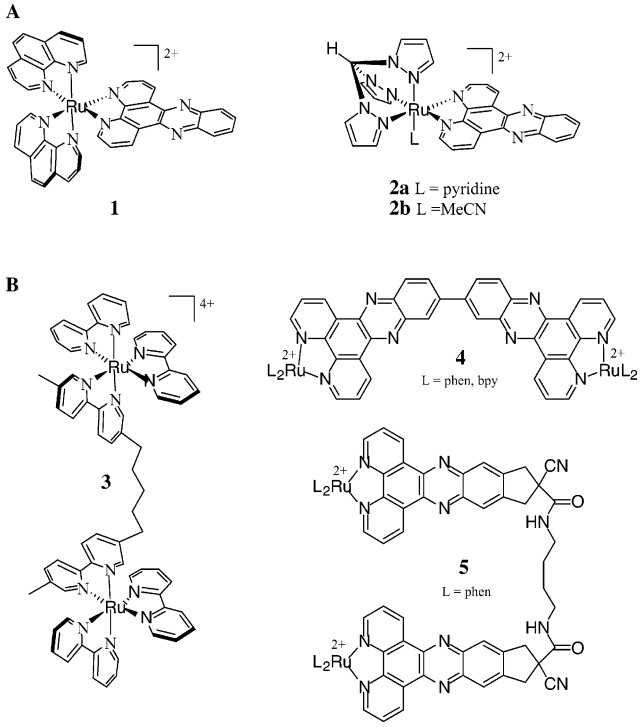

synthetic route to bis(metallo) intercalators. For example, using the readily available[8,11] $[Ru(tpm)(Cl)(dppz)]^+$ as a starting material, intercalating moieties can be linked via coordination to the metal centers using presynthesized tethers. Such a modular approach is attractive as systems containing a variety of linkers can be synthesized using a single methodology. However, for this initial report on the development of the new methodology, a single tether ligand, 4,4′dipyridyl-1,5-pentane, dpp, was chosen as a suitable linker.

Detailed here is the synthesis and preliminary studies on the DNA binding properties of a novel achiral bis(ruthenium) complex that contains two independent dppz intercalating ligands. The complex has been fully characterized using 2D NMR spectroscopy, and its DNA binding ability has been probed by spectroscopic titrations and isothermal titration calorimetry.

Experimental Section

Materials. Commercially available materials were used as received. Tris(1-pyrazolyl)methane,[12] 4,4′dipyridyl-1,5-pentane,[13] $[Ru(tpm)Cl_3]$,[11] and $[Ru(tpm)(dppz)Cl][Cl]$[8,11] were synthesized via literature procedures. Calf thymus DNA (CT-DNA) was purchased from Sigma chemical company and was purified until Abs 260 nm/Abs 280 nm was >1.9. Poly(dA)·poly(dT) and poly(dG)·poly(dC) DNA was purchased from Amersham Phamacia Biotech and was used as received. Concentrations of DNA solutions were determined spectroscopically using the following extinction coefficients. CT-DNA $\epsilon = 6600$ mol^{-1} dm^3 cm^{-1} at 260 nm, poly(dA)·poly(dT) $\epsilon = 6000$ mol^{-1} dm^3 cm^{-1} at 260 nm, and poly(dG)·poly(dC) $\epsilon = 7400$ mol^{-1} dm^3 cm^{-1} at 253 nm. The buffer used for titrations was 25mM NaCl, 5 mmol Tris, pH 7.0, made with doubly distilled water (Millipore).

Instrumentation. Electronic spectra were recorded on a Carey bio-3 UV−visible spectrophotometer. Emission spectra were recorded on a Hitachi fluorimeter. NMR spectra (400 MHz) were recorded on a Bruker instrument with offline data analysis performed on an IBM PC running Bruker win-NMR software. FAB mass spectra were obtained on a Kratos MS80 machine working in positive ion mode, with a *m*-nitrobenzyl alcohol matrix. ITC experiments were performed on a Microcal microcalorimeter at 25 °C with 25mM Tris buffer at pH 7.0 with data analysis performed on an IBM PC running Microcal's origin software.

Synthesis and Characterization. [TpmdppRudppz]Cl_2, [6]-[Cl_2]. [TpmClRudppz]Cl (450 mg, 0.59 mmol) and $AgNO_3$ (2.1 equiv, 1.22 mmol, 191 mg) were refluxed in 1:1 EtOH/water (100 cm^3) for 3 h. The solution was cooled and filtered through Celite to remove AgCl. The filtrate was returned to the flask along with dpp (10 equiv, 5.792 mmol, 1.31 g), and the mixture was refluxed for 10 h. After cooling, the solution was concentrated and NH_4PF_6 was added until the complex precipitated. After collection by filtration, the crude product was dissolved in acetone (5 cm^3). Bu_4-NCl was added to precipitate the product as a dichloride salt, which was collected by filtration and copiously washed with acetone to remove excess dpp. The red solid was dried in vacuo. Mass = 454 mg (66.6%). A small amount of the product was converted to its hexafluorophosphate salt for analysis. ^{1}H NMR (d_6-acetone): δ_H = 1.25 (m, 2H), 1.51 (m, 2H), 1.59 (m, 2H), 2.54 (m, 2H), 2.59 (m, 2H), 6.30 (t, 1H), 6.92 (dd, 1H), 6.98 (m, 4H), 7.23 (dd 2H), 7.61 (dd, 2H), 8.23 (m, 4H), 8.44 (dd, 2H), 8.46 (dd, 2H), 8.58 (m, 4H), 8.85 (dd, 2H), 9.42 (dd, 2H), 9.89 (dd, 2H), 9.91 (s, 1H). FAB−MS: *m*/*z* (%): 1114 (5) [M^+], 969 (40) [$M^+ - PF_6$], 824 (50) [$M^+ - 2PF_6$]. Accurate MS Anal. Calcd for $C_{43}H_{38}N_{12}PF_6Ru$ ($M^+ - PF_6$): 1114.1670. Found: 1114.1677.

[{TpmRudppz}$_2$dpp][PF_6]$_4$, [7][Cl_2]. [TpmClRudppz]Cl (100 mg, 0.13 mmol) and $AgNO_3$ (2.05 equiv, 42 mg, 0.264 mmol) were refluxed in 1:1 EtOH/water (30 cm^3) for 3 h. The cooled solution was filtered through Celite to remove AgCl. The filtrate was added dropwise to a refluxing solution of [**6**][Cl_2] (0.257 mmol, 230 mg) in 1:1 EtOH/water (30 cm^3). The solution was left to reflux for 3 days. The cooled solution was concentrated and chromatographed on Sephadex CM-C25 ion-exchange resin. The product was the first band eluted from the column with 0.1M NaCl in 5:3 water: acetone. The fractions containing the product were concentrated, and the product was precipitated by addition of NH_4PF_6. The product was collected by centrifugation, washed with water and Et_2O, and dried in vacuo. Mass = 43 mg (16.5%) of a red powder. ^{1}H NMR (d_6-acetone): δ_H = 1.19 (m, 2H), 1.40 (m, 4H), 2.44 (t, 4H), 6.28 (t, 2H), 6.89 (dd, 2H), 6.93 (m, 8H), 7.55 (dd 4H), 8.18 (dd, 4H), 8.24 (dd, 4H), 8.42 (dd, 4H), 8.57 (m, 6H), 8.86 (dd, 4H), 9.37 (dd, 4H), 9.86 (dd, 4H), 10.10 (s, 2H).). FAB−MS: *m*/*z* (%): 1858 (10) [M^+-PF_6], 857 (50) [M^{2+}-$2PF_6$]). Accurate MS Anal. Calcd for $C_{71}H_{58}N_{22}P_3F_{18}Ru_2$ ($M^+ - PF_6$): 1857.2227. Found: 1857.2277.

UV—Visible DNA Titrations A 3000 μL aliquot of a sample solution (15 μM) in a 1 cm path length quartz cuvette was loaded into the spectrometer sample block, maintained at 25 °C. Then 3000

(10) (a) Lincoln, P.; Nordén, B. *Chem. Commun*. **1995**, 214. (b) Önfelt, B.; Lincoln, P.; Nordén, B. *J. Am. Chem. Soc*. **1999**, *121*, 10846. (c) Önfelt, B.; Lincoln, P.; Nordén, B. *J. Am. Chem. Soc*. **2001**, *123*, 3630. (d) Wilhelmsson, L. M.; Westerland, F.; Lincoln, P.; Nordén, B. *J. Am. Chem. Soc*. **2002**, *124*, 12092.
(11) Llobet, A.; Doppelt, P.; Meyer, T. J. *Inorg. Chem.* **1993**, *27*, 514.
(12) Reger, D. L.; Grattan, T. C., Brown, K. J.; Little, C. A.; Lamba, J. J. S.; Rheingold, A. L.; Sommer, R. D. *J. Organomet. Chem*. **2000**, *607*, 120.
(13) Jampolsky, L. M.; Baum, M.; Kaiser, S.; Sternbach, L. H.; Goldberg, M. W. *J. Am. Chem. Soc.* **1952**, *74*, 5222.

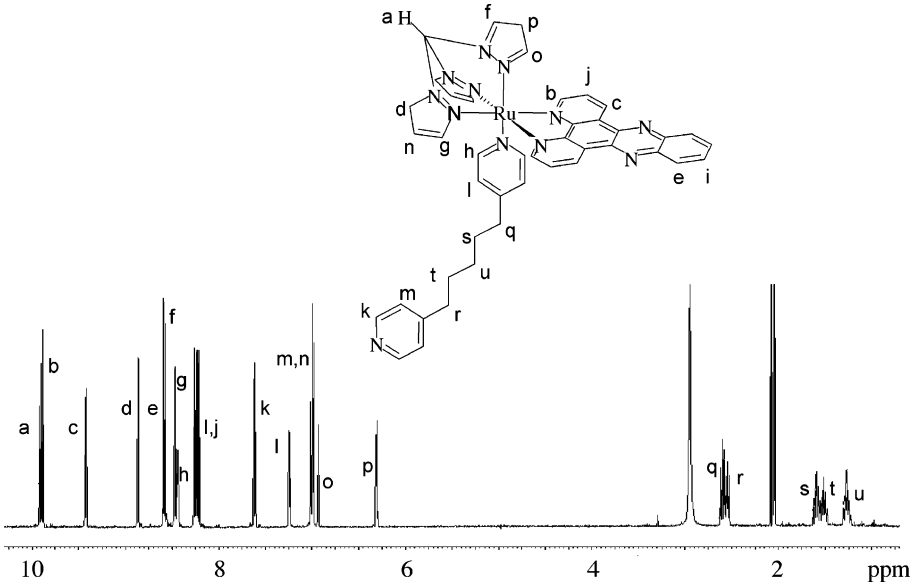

Figure 1. 400 MHz ^{1}H NMR spectrum of [**6**][$(PF_6)_2$] in acetonitrile.

μL of 5% buffer was placed in the reference cell of the spectrometer. After 30 min, to allow the cells to equilibrate, the first spectrum was recorded between 650 and 200 nm. Then, 2−5 μL of DNA solution was added to both the sample and reference cell, and each solution was thoroughly mixed. After another 30 min, the spectrum was taken again. The titration process was repeated until there was no change in the spectrum for at least four titrations indicating binding saturation had been achieved. Each titration was repeated at least three times.

Luminescence DNA Titrations. A 3000 μL aliquot of the sample solution in a 1 cm path length quartz cuvette was loaded into the fluorimeter sample block, maintained at 25 °C. After 30 min to allow the cell to equilibrate first spectrum was recorded. Then 2−5 μL of DNA solution (3−10 mM in base pairs) was then added to the sample cell, followed by thorough mixing. After 30 min, the spectrum was taken again. The titration process was repeated until there was no change in the spectrum for at least four titrations indicating binding saturation had been achieved. Each titration was repeated at least three times.

Isothermal Titration Calorimetry. Poly(dA)·poly(dT) and poly(dG)·poly(dC) dissolved in 2 mL of buffer (25 mmol NaCl, 5 mmol Tris·HCl, pH 7.0) and dialyzed against buffer for at least 24 h. In a typical experiment DNA (0.295 mM(bp)) was placed in the sample cell of the calorimeter and equilibrated to 25 °C. The metal complex (0.772 mM) was placed in the injection syringe and was injected into the sample cell in 19 15-μL injections after an initial 3 μL injection. Control titrations of buffer into buffer were also performed in order to determine background heats of dilution. The data were fitted to a single set of binding sites model using the Origin software package.

Results

Synthetic Studies. Previous work has shown that the axial chloride of [TpmRuCldppz][PF_6] is easily substituted by pyridine or nitrile ligands. However, these studies demonstrated that a 3-fold stoichiometric excess of pyridine ligand was needed in such reactions. Therefore, a two-step strategy for the synthesis of bimetallic complexes was investigated—Scheme 2.

First, [TpmRuCldppz]$^+$ was treated with $AgNO_3$ in the presence of excess dpp. This resulted in the dpp-substituted

Scheme 2. Synthesis of **6** and **7**

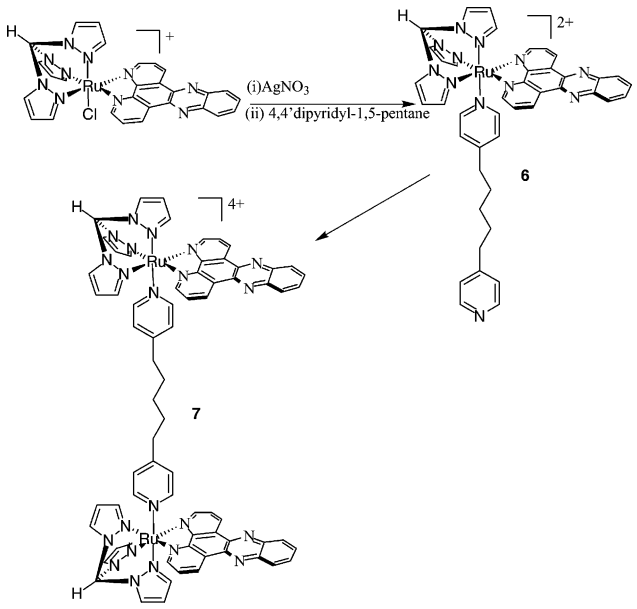

monomer **6**, isolated as an analytically pure solid by precipitation as its hexafluorophosphate salt. The bimetallic complex **7** was then synthesized by the reaction of [TpmRuCldppz]$^+$ with excess [**6**][Cl_2]. [**7**][$(PF_6)_4$] was isolated by cation exchange chromatography on Sephadex CM-C25 ion-exchange resin. Since sufficient material was produced for physical and bio-physical studies the yield of this reaction has yet to be optimized.

Spectroscopy Studies. In the absence of solid-state structural data for **7**, 1D and 2D ^{1}H NMR were used to fully structurally characterize the hexafluorophosphate salts of **6** and **7**. The 400 MHz 1D spectrum of **6** is shown in Figure 1.

The characteristic deshielded methane proton of the Tpm moiety is found as a singlet at 9.91 ppm (a). Cross-coupling analysis of the corresponding COSY spectrum reveals that the signals at 8.53, 6.30, and 6.92 ppm are the axially

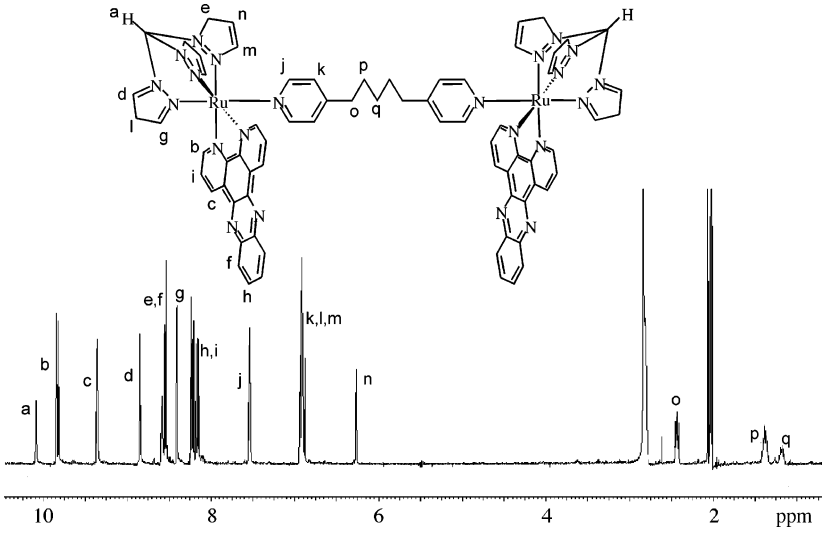

Figure 2. 400 MHz ^{1}H NMR spectrum of [**7**][$(PF_6)_2$] in acetonitrile.

coordinated pyrazole protons f, p, and o, respectively, while the resonances at 8.85, 6.99, and 8.46 ppm, are due to the equatorial coordinated pyrazole protons d, n, and g. The phenanthroline-type protons of dppz appear at 9.89 (b), 8.23 (j), and 9.42 ppm (c), with all three signals integrating to two protons each, while the protons in the phenazine region of the ligand appear at 8.55 (e) and 8.25 ppm (i). Due to coordination of one of the pyridine moieties of dpp to the ruthenium center, all seven sets of protons on this ligand are rendered inequivalent. The large coupling constant for the resonances at 8.44 (h) and 7.61 ppm (k) indicate that these protons reside adjacent to ring nitrogens, and the one with the largest downfield shift is assigned to the pyridyl ring coordination to the ruthenium. The other aromatic protons appear at 7.23 (l) and 7.02 ppm (m). The two closely positioned triplets at 2.60 and 2.55 ppm and are protons q and r on the alkyl linker, while protons s and t appear as multiplets at 1.59 and 1.52 ppm. The central alkyl proton u appears as a multiplet at 1.26 ppm.

The 400 MHz 1D spectrum of [**7**][PF_6]$_2$ is shown in Figure 2. Again the methyl proton, a, of Tpm is found as a sharp singlet at 10.10 ppm. The axial pyrazole protons are assigned to the signals at 8.60 (e), 6.28 (n), and 6.89 ppm (m), which all integrate to two protons each. The equatorial pyrazole protons can be found at 8.86 (d), 6.93 (l), and8.42 ppm (g) and integrate to four protons each. Analysis of cross-coupling from the corresponding COSY spectrum shows that the phenanthroline-type dppz protons appear at 9.85 (b, $J = 9$ Hz), 8.17 (i), and 9.37 ppm (c). The phenazine-type protons appear at 8.55 ppm (f), and they are coupled to the proton at 8.24 ppm (h). The formation of the bimetallic species means that the dpp linker ligand now displays higher symmetry, resulting in a simplification of its signals, for example, the aromatic protons now appear as only two signals at 7.55 ppm (j, $J = 9$ Hz) and ca. 6.00 ppm (k). This latter signal is not fully resolved as it is superimposed on pyrazole proton l.

A comparison of the key signals in the 1D NMR of both [**6**][$(PF_6)_2$] and [**7**]][$(PF_6)_4$] provides further evidence for the formation of the bimetallic complex. First, in the monometallic complex **6** the integral ratio of the methyl proton of tpm (a) to the central methylene proton (u) of the linker ligand is 1:2. However, for **7** the ratio a:q is 2:2, indicating two Tpm ligands, and thus two ruthenium centers are present for each linker. Second, for **6**, the five alkyl signals and four pyridyl signals from the dipyridyl linker all give separate resonances due to the asymmetric coordination of ruthenium to only one of the pyridines. In the bimetallic complex however, there are only three resonances with ratios 4:4:2 in the alkyl region and two resonances with ratios 4:4 for the pyridyl protons of dpp. This indicates the symmetric coordination of each of the pyridines of dpp to an identical ruthenium center. Furthermore, FAB and accurate mass spectroscopy, as well as elemental analysis, are all consistent with the structures assigned by these NMR studies

Table 1. Photophysical Properties of the Reported Complexes

	absorption[a]			emission[a]		
complex	λ_{max}/nm	ϵ/mol^{-1} dm^3 cm^{-1}	assignt	λ_{ex}/nm	λ_{em}/nm	assignt
6	279	44039	$\pi \rightarrow \pi^*$	450	624	MLCT
	317	16202	$\pi \rightarrow \pi^*$			
	348	17559	$\pi \rightarrow \pi^*$			
	397	6883	$\pi \rightarrow \pi^*$			
	470	2363	MLCT			
7	279	163997	$\pi \rightarrow \pi^*$	450	672	MLCT
	317	50718	$\pi \rightarrow \pi^*$			
	351	53251	$\pi \rightarrow \pi^*$			
	399	20192	$\pi \rightarrow \pi^*$			
	470	6982	MLCT			

[a] Hexafluorophosphate salts recorded in acetonitrile.

Photophysical Studies. The UV−visible spectra of the complexes recorded in acetonitrile solution show characteristic absorptions for ruthenium(II) diimine complexes; see Table 1. Both **6** and **7** show the characteristic double humped absorption due to transitions involving the dppz ligand at 348, 397 nm for [**6**][$(PF_6)_2$] and 351, 399 nm for [**7**][$(PF_6)_4$] and a broad Ru(dπ) $\rightarrow$ dppz(π^*) MLCT at 470 nm. High energy $\pi \rightarrow \pi^*$ transitions are very similar for both **6** and **7**, except transitions are much more intense in the bimetallic species than in the monometallic species (ϵ (279) = 163997 and 44039 mol^{-1} dm^3 cm^{-1}, respectively).

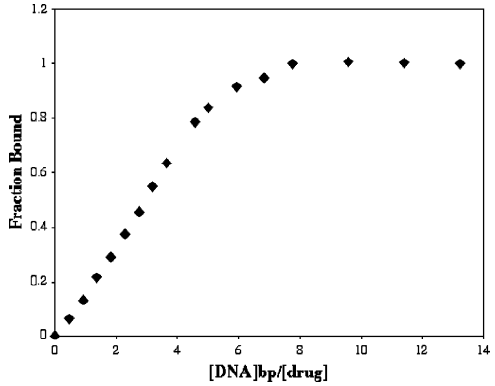

Figure 3. Typical binding curve obtained from emission titration of [**6**]-$[Cl_2]$ with CT-DNA in 25 mmol of NaCl and 5 mmol of Tris−HCl, pH 7.0, 25 °C.

In acetonitrile solution, [**6**][$(PF_6)_2$] and [**7**][$(PF_6)_4$] show characteristic[5−7] emission from the Ru(dπ) → dppz(π*) MLCT; see Table 1. However, emission from **7** is noticeably less intense than that from **6** and is significantly red-shifted (672 nm compared to 624 nm in the monometallic). This phenomenon has also been observed in other related bimetallic systems and is indicative of self-quenching due to the close proximity of the linked metal centers.[14,15] More detailed photophysical studies inspired by these observations are currently underway.

DNA Binding Studies. The water-soluble chloride salts [**6**][Cl_2] and [**7**][Cl_4] were obtained via anion metathesis of their respective hexafluorophosphate salts using ^{n}Bu$_4$NCl in acetone. The interaction of these complexes with calf thymus DNA (CT-DNA) in aqueous buffer (25mM NaCl, 5 mmol Tris, pH 7.0) was investigated using UV−visible and emission spectroscopic titrations.

The addition of CT-DNA to solutions of **6** results in characteristically large hypochromicity in both MLCT and $\pi \rightarrow \pi^*$ absorption bands. There is also an appreciable bathochromic shift of one of the high-energy bands, from 275 to 292 nm. Emission titrations were accompanied by the expected DNA "light switch" effect: aqueous solutions of [**6**][Cl_2] are nonluminescent, until addition of CT-DNA results in Ru(dπ) → dppz(π*) MLCT emission at 651 nm. This raw data produced typical saturation binding curves, Figure 3. All these observations are consistent with the interaction of a metallo-intercalator and DNA.[4−7,10]

Fits of these data to the McGhee−Von Hippel (MVH) model[16] indicate that **6** binds to CT-DNA with a $K_b = 3.5 \times 10^5$ mol^{-1} dm^3 and a site size, *S*, of ca. 4.47 base pairs. Previous binding studies on the related complexes **2a** and **2b** have revealed lower site sizes ($S \approx 3$),[8] suggesting that the more bulky dpp ligand is responsible for the relative increase in *S* and the lower binding affinity (K_b for **2a** and **2b** $\geq 10^6$).

The interaction of [**7**][Cl_4] with CT-DNA also results in changes in absorption and emission but, unlike a related Re^I system, linked with a shorter tether,[15] the binding is monophasic. However, although the hypochromicity observed for the dimer is comparable to that seen for **6**, Figure 4, enhancement of the luminescence is less pronounced with intensities being 60−65% of that seen for the monomeric analogue at the same concentration. This, again, is consistent with self-quenching—although, the possibility that it is indicative of differences in DNA binding modes cannot be ruled out—vide infra. Fitting of the data to the MVH model revealed that the binding affinity of **7** is of the same order as that **6**, while the apparent site size is actually lower. Attempts to fix the site-size at higher values of *S* resulted in poorer data fits. It is known that MVH fits for potentially bis-intercalating systems often produce anomalously low *S* values, particularly when there is significant contribution from mono-intercalative binding modes.[17] An observation that may be relevant in this case, vide infra.

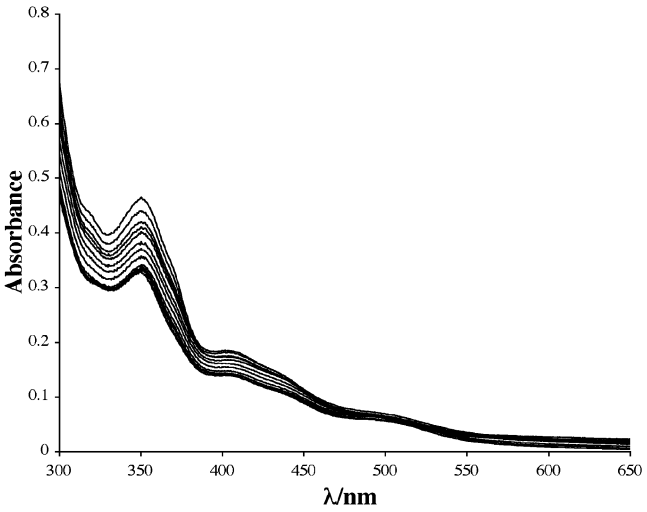

Figure 4. Absorption spectral changes of complex **7** in aqueous buffer upon addition of CT-DNA.

Isothermal Titration Calorimetry Studies. To further investigate the properties of the dimer, binding of **6** and **7** to DNA homopolymers was compared using isothermal titration calorimetry, ITC.[18]

The interaction of [**6**][Cl_2] with poly(dA)·poly(dT), Figure 5a and Table 2, can be compared to analogous data previously obtained from studies on **1**[19] and **2b**.[8] In all three cases, the thermodynamic profile for binding displays positive enthalpy and entropy changes indicating that, like **1** and **2**, intercalative binding by **6** is dominated by hydrophobic interactions.[19]

The interaction of [**7**][Cl_4] with Poly(dA)·poly(dT), fits well to a single set of identical binding sites model, Figure 5b and Table 2. Additionally, the resultant *S* value is larger than that obtained from the MVH analysis, being closer to values observed for related linked chromophoric systems.[9,10b,c,20]

(14) Juris, A.; Balzani, V.; Barigelletti, F.; Campagna, S.; Belser, P.; von Zelewsky, A. *Coord. Chem. Rev.* **1988**, *84*, 85.
(15) Metcalfe, C.; Webb, M.; Thomas, J. A. *Chem. Commun.* **2002**, 2026.
(16) McGhee, J. D.; von Hippel, P. H. *J. Mol Biol.* **1974**, *86*, 469.
(17) (a) Shafer, R. H.; Waring, M. J. *Biopolymers* **1980**, *19*, 431. (b) Shafer, R. H.; Waring, M. J. *Biopolymers* **1982**, *21*, 2279.
(18) (a) Haq, I.; Chowdhry, B. Z.; Jenkins, T. C. *Methods Enzymol.* **2001**, *340*, 109. (b) Ladbury, J. E.; Chowdhry, B. Z. *Chem. Biol.* **1996**, *3*, 791 (c) Jelesarov, I.; Bosshard, H. R. *J. Mol. Recognit.* **1999**, *12*, 791.
(19) Haq, I.; Lincoln, P.; Suh, D.; Nordén, B.; Chowdrey, B. Z.; Chaires, J. B. *J. Am. Chem. Soc.* **1994**, *117*, 4788.
(20) Leng, F.; Priebe, W.; Chaires, J. B. *Biochemistry* **1998**, *37*, 1743.

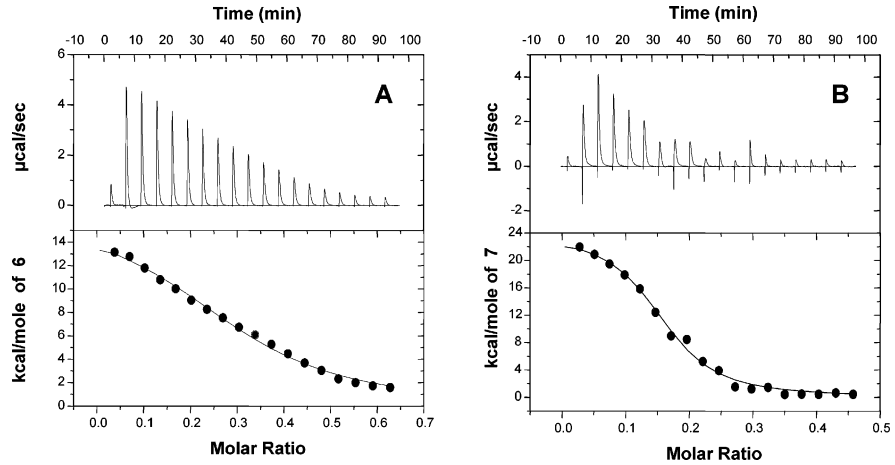

Figure 5. (A) Raw ITC data for the interaction of 0.9 mM [**6**][Cl_2] with 0.3 mM(bp) of poly(dA)poly(dT) at 25 °C in a 5 mM Tris−HCl, 25 mM NaCl pH 7.00 buffer. These peaks were integrated with respect to time and corrected for heats of ligand dilution in order to obtain the enthalpy data in the bottom panel. This binding isotherm was fit using a single-site binding model. (B) Analogous data for the interaction of [**7**][Cl_4].

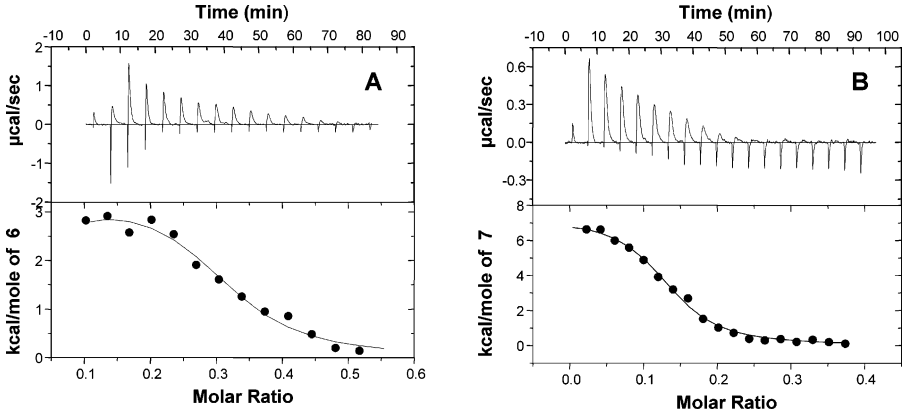

Figure 6. (A) Raw ITC data for the interaction of 0.9 mM [**6**][Cl_2] with 0.3 mM(bp) of poly(dG)poly(dC) at 25 °C in a 5 mM Tris−HCl, 25 mM NaCl, pH 7.00 buffer. These peaks were integrated with respect to time and corrected for heats of ligand dilution in order to obtain the enthalpy data in the bottom panel. There were insufficient data points during the first phase of the binding curve and so fits to a two-site model were unreliable. The first two data points were therefore removed and the resultant isotherm was fit to a single site binding model. (B) Analogous data for the interaction of [**6**][Cl_4].

Table 2. Thermodynamic Parameters for the Interaction of [**6**][Cl_2] and [**7**][Cl_4] with Poly(dA)·Poly(dT) and Poly(dG)·Poly(dC) Obtained via ITC

complex	K_b/M(bp)$^{-1}$	S/bp	ΔH/kcal mol^{-1}	ΔG/kcal mol^{-1}	$T\Delta S$/kcal mol^{-1}
			poly(dA)·poly(dT)		
6	$(2.5 \pm 0.8) \times 10^5$	3.3	$+3.3 \pm 0.3$	-7.36 ± 0.3	$+10.66 \pm 1.8$
7	$(4.4 \pm 0.6) \times 10^5$	7.6	$+7.3 \pm 0.2$	-7.69 ± 0.3	$+14.99 \pm 2.6$
			poly(dG)·poly(dC)		
6	$(4.6 \pm 0.5) \times 10^5$	3.2	$+16.4 \pm 1.6$	-7.72 ± 0.5	$+24.12 \pm 2.7$
7	$(4.2 \pm 0.6) \times 10^5$	6.4	$+23.8 \pm 2.6$	-7.67 ± 0.3	$+31.47 \pm 3.5$

In contrast, the K_b value obtained does correlate well with that obtained from the luminescent studies on CT-DNA, confirming that there is very little (if any) enhancement of binding affinity. Again, the binding is also associated with positive enthalpy and entropy changes. However, while the positive enthalpic contribution has doubled compared to the data for **6**, there is a smaller relative increase in the $T\Delta S$ contribution, thus there is very little change in the overall free energy of binding.

The interaction of **6** with Poly(dG)·poly(dC), Figure 6a, can be compared to analogous data previously obtained from studies on **2a** where, after saturation of a few high-affinity sites, intercalative binding was observed. The data obtained for **6**, Table 2, result in values of K_b and S that are similar to those obtained for **2a**, where $K_b = 1.1 \times 10^6\ M^{-1}$, $S = 2.8$.

Compared to poly(dA)·poly(dT), the interaction of **6** with poly(dG)·poly(dC) involves much larger positive enthalpic and entropic contributions. These data also contrast strongly with those obtained for **2a** where an analogous study revealed a pronounced binding preference to GC sequences, driven by an exothermic process with a much lower $T\Delta S$ contribution.

In contrast, data obtained from the interaction of **7** with poly(dG)·poly(dC) fit well to a single set of identical binding sites model and, although S is larger than that of the monomer, it is lower than that observed with poly(dA)·poly-

(dT)—Figure 6b. This is slightly surprising as poly(dG)·poly(dC) is structurally related to the more compact A-form.

7 shows no specificity with affinities for poly(dG)·poly(dC) and poly(dA)·poly(dT) being almost identical and K_b of the bimetallic complex is almost the same as, if not slightly lower than, that of **6**. As is the case for the interaction with poly(dA)·poly(dT), a larger positive enthalpic contribution to the binding of **7** is accompanied by smaller increase in $T\Delta S$ contribution, thus leading to very little change in the overall free energy of binding relative to the data obtained for **6**.

Discussion

Luminescence and ITC titrations indicate that, while **6** and **7** bind relatively avidly to DNA, there are significant differences in these interactions compared with those observed for simpler monometallic systems.

The generally lowered binding affinity of **6** seems to be due to the increased steric bulk of the dpp ligand. Effects such as these have been observed for other metallo-intercalators containing sterically demanding ancillary ligands.[21] More particularly, coordination of the dpp ligand also results in a concomitant loss in binding specificity as, unlike **2b**, **6** shows little binding preference for GC sequences. It seems that coordination of dpp prevents the $[Ru^{II}(tpm)(dppz)]^{2+}$ moiety from making the specific interactions required for such binding.

The binding parameters of **7** are particularly distinctive. Simple arguments dictate that binding constants for bis-intercalators should be the square of their monomeric analogues.[22] Although real systems have not shown such large enhancements, significant increases in affinities have been observed.[10,20] The observation of the light-switch effect for **7** is a clear indication of intercalation: previous studies have concluded that this phenomenon demands embedding of the phenazine moiety of the dppz ligand deep into the DNA helix.[5c] Given this fact, the ITC data and the anomalous McGhee−von Hippel fit suggest that **7** is not a true bis-intercalator and only one chromophore intercalates. Furthermore, there is no evidence of biphasic interstrand binding that has been observed in a related system containing a shorter tether.[15] Surprisingly, a comparison of the binding parameters for **7** with those of structurally analogous, but known nonintercalators reveals a striking similarity: K_b for **3** $= 2.4 \times 10^5\ M^{-1}$, $S = 6.4$ with CT-DNA.[9b] To further investigate this issue, synthesis of systems with longer tethers are underway.

An alternative explanation involves an analysis of the thermodynamic data obtained by ITC. It is known that binding in metallo-intercalators is entropically driven. However, relative to **6**, the data for **7** only show a modest increase in the $T\Delta S$ contribution. Binding of tethered systems can result in a considerable loss in the degrees of freedom available to the linker, leading to a unfavorable entropic contribution to binding.[20] Thus, as has been suggested before,[23] it may that the comparative flexibility of the tether is directly responsible for the comparatively low free energy of binding.

Further biophysical studies that will provide more detail on the nature of the interaction of **6** and **7** with DNA, are underway. The synthesis of related mono- and oligometallic systems designed to show specific high affinity binding characteristics are also being investigated.

Acknowledgment. We gratefully acknowledge the support of The Royal Society (J.A.T.) and EPSRC (C.M., I.H., and J.A.T.).

Supporting Information Available: Figures showing 2D COSY ^{1}H NMR spectra of [**6**][$(PF_6)_2$] and [**7**][$(PF_6)_4$]. This material is available free of charge via the Internet at http://pubs.acs.org.

IC034749X

(21) See for example; (a) Carson, D. L.; Huchital, D. H.; Mantilla, E. J.; Sheardy, R. D.; Murphy, W. R. *J. Am. Chem. Soc*. **1993**, *115*, 6424. (b) Liu, J.-G.; Zhang, Q.-L.; Shi, X.-F., Ji, L.-N. *Inorg. Chem.* **2001**, *40*, 5045.

(22) Wakelin, L. P. G. *Med. Res. Rev.* **1986**, *6*, 275.

(23) Mammen, M.; Chi, S.-K.; Whitesides, G. M. *Angew. Chem., Int. Ed*. **1998**, *37*, 2754.